AIAA JOURNAL
Vol. 38, No. 2, February 2000

Three-Dimensional Asymptotic Analysis of Multiple-Electroded Piezoelectric Laminates

Zhen-Qiang Cheng*
University of Science and Technology of China, 230026 Hefei, Anhui, People's Republic of China
and
R. C. Batra†
Virginia Polytechnic Institute and State University, Blacksburg, Virginia 24061

The problem of piezoelectric laminates with specified surface tractions and surface and internal electric potentials is studied. By writing the governing equations in the state-space formulation, employing an asymptotic expansion technique, and expressing electric displacement jumps across internal electrodes in terms of basic unknowns, the three-dimensional problem is reduced to a hierarchy of two-dimensional equations with the same homogeneous operators for each order. Different nonhomogeneous terms are only related to the preceding-order solution and can be readily determined by recurrence relations. Moreover, for pure elasticity, the present field equations of the leading order represent the classical thin elastic plate model. The proposed formulation is illustrated by considering a rectangular piezoelectric plate made of an orthotropic material, and with its edges simply supported and grounded. The convergence of the solution is discussed and the repeated averaging technique for partial sums is used to accelerate the convergence of the series solution. Computed results are found to agree well with available analytical results, and new results for electromechanically coupled problems are presented.

I. Introduction

A smart structural system is a multifunctional unit involving active materials for performing the operations of distributed modeling, sensing, and control of passive load-bearing structures.[1–8] Integrated active materials are comprised of piezoelectric patches and layers that act as sensors and actuators. Because of their compact size and light weight, a great number of piezoelectric elements can be used without significantly changing the structural properties of the entire system. However, the structure does become more brittle.

Analogous to the two-dimensional approaches for constructing equivalent single-layer plate and shell theories of elastic laminates, various piezoelectric plate and shell theories[9–15] have been proposed. These theories assume the same forms of the overall through-thickness distributions of mechanical displacements as those in the classical and shear deformation elastic plate and shell theories. However, these theories are not very accurate even for purely elastic laminates as transverse tractions do not generally satisfy the continuity conditions at the layer interfaces.[16,17]

To develop consistent two-dimensional theories for elastic laminates, asymptotic approaches[18–25] have been used to reduce three-dimensional field equations to two-dimensional equations that can be successively solved in a systematic manner. The leading-order approximation of an asymptotic theory for thin single-layer piezoelectric plates[26,27] has also been proposed.

By extending the work[28,29] for simply supported elastic laminates, exact solutions for simply supported laminated piezoelectric plates[30–32] were given. Transfer matrix approaches[33–38] were developed to study the electromechanical coupling characteristics of laminated piezoelectric plates. In the conventional transfer matrix description for a multiple-layer stack, the displacements, out-of-plane stresses, electric potential and transverse electric displacement are chosen as the termination parameters because they are continuous across layer interfaces. Thus the interfacial continuity conditions can be easily satisfied. However, for a structural element with internal conducting electrodes, the normal electric displacement must be different on the two sides of an electroded surface. In this case the transfer matrix description must be modified to accommodate the discontinuity in the normal electric displacement.[33]

Here, we present an asymptotic expansion method for the analysis of piezoelectric laminates with surface and internal electrodes. The transfer matrix formulation is given in a compact form by using the tensor notation. By expressing transverse electric displacement jumps across internal electrodes in terms of basic unknowns, we provide a hierarchy of two-dimensional problems whose solution determines the solution of the given three-dimensional problem. These two-dimensional problems can be easily solved when boundary-layer effects are negligible. Results for three example problems are presented. These establish the validity and accuracy of the present approach, and also point out some deficiencies in the two-dimensional models.

II. State-Space Equations

We consider an undeformed laminated plate of uniform thickness h in a rectangular Cartesian coordinate system $\{x_i\}(i = 1, 2, 3)$, with the lower plane of the plate coinciding with $x_3 = 0$. The plate is composed of different homogeneous monoclinic piezoelectric materials. Hereafter, a comma followed by a subscript i denotes the partial derivative with respect to x_i, and a repeated index implies summation over the range of the index with Latin indices ranging from 1 to 3 and Greek indices from 1 to 2.

In the absence of body force and electric charge density, the field equations of elastic equilibrium and Gauss's law of electrostatics are[39,40]

$$\tau_{ij,j} = 0, \qquad D_{i,i} = 0 \tag{1}$$

where τ_{ij} is the stress tensor and D_i the electric displacement. The infinitesimal strain tensor S_{kl} and electric field E_k are related to the mechanical displacements u_k and the electric potential φ through the gradient relations

$$S_{kl} = \tfrac{1}{2}(u_{k,l} + u_{l,k}), \qquad E_k = -\varphi_{,k} \tag{2}$$

Equations (1) and (2) are supplemented by the following constitutive relations for a linear piezoelectric body:

$$\tau_{ij} = c_{ijkl} S_{kl} - e_{kij} E_k, \qquad D_i = e_{ikl} S_{kl} + \varepsilon_{ik} E_k \tag{3}$$

Received 10 August 1998; revision received 15 April 1999; accepted for publication 22 June 1999.

*Associate Professor, Department of Modern Mechanics; currently Visiting Research Associate, Department of Engineering Science and Mechanics, Virginia Polytechnic Institute and State University, Blacksburg, VA 24061.
†Clifton C. Garvin Professor, Department of Engineering Science and Mechanics.

Here c_{ijkl} is the fourth-order elasticity tensor measured at a constant electric field, e_{kij} the third-order piezoelectric tensor, and ε_{ik} the second-order dielectric tensor measured at a constant strain. These material moduli exhibit the following symmetries:

$$c_{ijkl} = c_{jikl} = c_{klij}, \qquad e_{kij} = e_{kji}, \qquad \varepsilon_{ik} = \varepsilon_{ki} \tag{4}$$

The constitutive relations for monoclinic piezoelectric materials whose material properties are symmetric with respect to reflections in the midplane can be written as

$$\begin{aligned}
\tau_{\alpha\beta} &= c_{\alpha\beta\omega\rho} S_{\omega\rho} + c_{\alpha\beta 33} S_{33} - e_{3\alpha\beta} E_3 \\
\tau_{\alpha 3} &= 2c_{\alpha 3\omega 3} S_{\omega 3} - e_{\omega\alpha 3} E_\omega \\
\tau_{33} &= c_{33\omega\rho} S_{\omega\rho} + c_{3333} S_{33} - e_{333} E_3 \\
D_\alpha &= 2e_{\alpha\omega 3} S_{\omega 3} + \varepsilon_{\alpha\omega} E_\omega \\
D_3 &= e_{3\omega\rho} S_{\omega\rho} + e_{333} S_{33} + \varepsilon_{33} E_3
\end{aligned} \tag{5}$$

The numbers of nonzero independent elastic, piezoelectric, and dielectric moduli are, respectively, 13, 8, and 4 for a monoclinic material. The material moduli are taken to be piecewise constant functions of x_3 for the laminated plate. To develop an efficient and analytical methodology for accurate and reliable investigation of three-dimensional deformations of smart plates, the preceding equations are written in a state space as

$$\partial_z \begin{bmatrix} \boldsymbol{F} \\ \boldsymbol{G} \end{bmatrix} = \varepsilon \begin{bmatrix} \boldsymbol{0} & \boldsymbol{A} \\ \boldsymbol{B} & \boldsymbol{0} \end{bmatrix} \begin{bmatrix} \boldsymbol{F} \\ \boldsymbol{G} \end{bmatrix} \tag{6}$$

where we have scaled the thickness coordinate $x_3 = \varepsilon z$ by the small parameter $\varepsilon = h/a$ with a being a typical in-plane dimension. Thus $\varepsilon\partial/\partial x_3 = \partial/\partial z \equiv \partial_z$, and z varies from 0 to a as x_3 goes from 0 to h. Furthermore,

$$\boldsymbol{F} = \begin{bmatrix} u_1 \\ u_2 \\ \tau_{33} \\ D_3 \end{bmatrix}, \qquad \boldsymbol{G} = \begin{bmatrix} \tau_{13} \\ \tau_{23} \\ u_3 \\ \varphi \end{bmatrix} \tag{7}$$

The 4×4 operator matrices $\boldsymbol{A}$ and $\boldsymbol{B}$ contain the in-plane differential operator $\partial_\alpha \equiv \partial/\partial x_\alpha$ and depend on z only through the material moduli:

$$\boldsymbol{A} = \begin{bmatrix} \boldsymbol{I} & -\boldsymbol{J}_\beta \partial_\beta \\ -\boldsymbol{J}_\beta^T \partial_\beta & \boldsymbol{K}_{\beta\rho} \partial_\beta \partial_\rho \end{bmatrix}, \qquad \boldsymbol{B} = \begin{bmatrix} -\boldsymbol{L}_{\beta\rho} \partial_\beta \partial_\rho & -\boldsymbol{M}_\beta \partial_\beta \\ -\boldsymbol{M}_\beta^T \partial_\beta & \boldsymbol{N} \end{bmatrix} \tag{8}$$

where both $\boldsymbol{A}$ and $\boldsymbol{B}$ have been partitioned into four 2×2 operator submatrices. The elements of matrices $\boldsymbol{I}$ and $\boldsymbol{N}$ are defined by

$$\boldsymbol{I} = (I^{\omega\alpha}) = (c^{-1}_{\omega 3 \alpha 3}) = \frac{1}{c_{1313}c_{2323} - c_{1323}^2} \begin{bmatrix} c_{2323} & -c_{1323} \\ -c_{1323} & c_{1313} \end{bmatrix}$$

$$\text{or} \qquad (c_{\alpha 3 \omega 3}) = \begin{bmatrix} c_{1313} & c_{1323} \\ c_{1323} & c_{2323} \end{bmatrix}$$

$$\boldsymbol{N} = (N^{\alpha\omega}) = \frac{1}{c_{3333}\varepsilon_{33} + e_{333}^2} \begin{bmatrix} \varepsilon_{33} & e_{333} \\ e_{333} & -c_{3333} \end{bmatrix}$$

$$\text{or} \qquad N^{-1} = \begin{bmatrix} c_{3333} & e_{333} \\ e_{333} & -\varepsilon_{33} \end{bmatrix} \tag{9}$$

$\boldsymbol{J}_\beta$ and $\boldsymbol{M}_\beta$ are matrices with each of their elements being a vector defined by

$$\begin{aligned}
\begin{bmatrix} J_\beta^{\omega 1} & J_\beta^{\omega 2} \end{bmatrix} &= \begin{bmatrix} \delta_{\omega\beta} & I^{\omega\alpha} e_{\beta\alpha 3} \end{bmatrix} \\
\begin{bmatrix} M_\beta^{\alpha 1} & M_\beta^{\alpha 2} \end{bmatrix} &= \begin{bmatrix} c_{\alpha\beta 33} & e_{3\alpha\beta} \end{bmatrix} \boldsymbol{N}
\end{aligned} \tag{10}$$

and $\boldsymbol{K}_{\beta\rho}$ and $\boldsymbol{L}_{\beta\rho}$ are matrices with each of their elements being a tensor and

$$\begin{aligned}
K_{\beta\rho}^{11} = K_{\beta\rho}^{12} = K_{\beta\rho}^{21} = 0, \qquad K_{\beta\rho}^{22} &= J_\beta^{\omega 2} e_{\rho\omega 3} + \varepsilon_{\beta\rho} \\
L_{\beta\rho}^{\alpha\omega} &= c_{\alpha\beta\omega\rho} - M_\beta^{\alpha 1} c_{33\omega\rho} - M_\beta^{\alpha 2} e_{3\omega\rho}
\end{aligned} \tag{11}$$

Here $\delta_{\alpha\beta}$ is the Kronecker delta and we have used superscripts, to which the conventional summation also applies, to denote the row and column indices of a matrix element. The subscripts of the corresponding element, which is a vector or a tensor, imply the usual components of a tensor. These submatrices are only related to the material moduli depending on x_3. The in-plane stresses and in-plane electric displacements, which may be discontinuous in x_3, are given by

$$\begin{aligned}
\tau_{\alpha\beta} &= \begin{bmatrix} L_{\beta\rho}^{\alpha 1}\partial_\rho & L_{\beta\rho}^{\alpha 2}\partial_\rho & M_\beta^{\alpha 1} & M_\beta^{\alpha 2} \end{bmatrix} \boldsymbol{F} \\
D_\rho &= \begin{bmatrix} J_\rho^{12} & J_\rho^{22} & 0 & -K_{\beta\rho}^{22}\partial_\beta \end{bmatrix} \boldsymbol{G}
\end{aligned} \tag{12}$$

In the absence of internal electrodes, $\boldsymbol{F}$ and $\boldsymbol{G}$ must be continuous across each interface layer.

III. Asymptotic Approach

The general problem of piezoelectricity is to determine the global and local electroelastic fields under applied mechanical and electric loading. In this paper the mechanical loading is specified by the tangential tractions $q_\alpha^\pm$ and the normal pressures $q_3^\pm$ imposed on the top and bottom plate surfaces, whereas the electric loading is specified by applied potentials. Specifically, the two bounding surfaces and r electroded interfaces of the plate are coated with very thin conducting electrodes. These electrodes may carry an alternating forcing potential. For simplicity, the thickness of each electrode is neglected, and it is modeled as a mathematical surface with a specified electric potential. The distance between the ith internal electrode surface and the bottom-most surface of the plate is ${}^{(i)}a$. In particular, we set ${}^{(0)}a = 0$ and ${}^{(r+1)}a = a$ for the position of the bottom most and top most surfaces. The electroded surface at $z = {}^{(i)}a$ is subjected to the electric potential ${}^{(i)}V$ $(i = 0, \ldots, r+1)$. This physical model includes the important cases of a laminated plate with sensors and actuators bonded to its topmost and bottommost surfaces and of a laminated plate with embedded sensors and actuators.

For general mechanical loading conditions (excluding the particular case where the tractions on the top and bottom surfaces are equal), the transverse shear stresses are of the order $\mathcal{O}(\varepsilon^2)$, and the transverse normal stress is of the order $\mathcal{O}(\varepsilon^3)$, as in the case of pure elasticity.[18] These surface forcing functions are then scaled as

$$\tau_{\alpha 3}(x_\rho, 0) = \varepsilon^2 q_\alpha^-(x_\rho), \qquad \tau_{\alpha 3}(x_\rho, a) = \varepsilon^2 q_\alpha^+(x_\rho) \tag{13}$$

$$\tau_{33}(x_\rho, 0) = -\varepsilon^3 q_3^-(x_\rho), \qquad \tau_{33}(x_\rho, a) = -\varepsilon^3 q_3^+(x_\rho) \tag{14}$$

The electric potential is constructed to be of the order $\mathcal{O}(\varepsilon^2)$, i.e.,

$$\varphi[x_\rho, {}^{(i)}a] = \varepsilon^2 \, {}^{(i)}V(x_\rho) \qquad (i = 0, \ldots, r+1) \tag{15}$$

To find solutions of successive approximations, we express the state-space functions $\boldsymbol{F}$ and $\boldsymbol{G}$ in the form of a regular expansion in terms of the small parameter ε as

$$\begin{bmatrix} \boldsymbol{F} \\ \boldsymbol{G} \end{bmatrix} = \sum_{n=0}^{\infty} \varepsilon^{2n} \begin{bmatrix} \varepsilon \boldsymbol{f}^{(n)} \\ \boldsymbol{g}^{(n)} \end{bmatrix} \tag{16}$$

Then the surface traction conditions (13) and (14) and the electric potential conditions (15) for surface and internal electrodes may be expressed by the components of the expansion terms of $\boldsymbol{F}$ and $\boldsymbol{G}$. For the leading order

$$g_\alpha^{(0)}(0) = \tau_{\alpha 3}^{(0)}(0) = 0, \qquad g_\alpha^{(0)}(a) = \tau_{\alpha 3}^{(0)}(a) = 0 \tag{17}$$

$$f_3^{(0)}(0) = \tau_{33}^{(0)}(0) = 0, \qquad f_3^{(0)}(a) = \tau_{33}^{(0)}(a) = 0 \tag{18}$$

$$g_4^{(0)}[{}^{(i)}a] = \varphi^{(0)}[{}^{(i)}a] = 0 \qquad (i = 0, \ldots, r+1) \tag{19}$$

and for the remaining orders

$$g_\alpha^{(n+1)}(0) = \tau_{\alpha 3}^{(n+1)}(0) = q_\alpha^- \delta_{n0} \tag{20a}$$

$$(n \geq 0)$$

$$g_\alpha^{(n+1)}(a) = \tau_{\alpha 3}^{(n+1)}(a) = q_\alpha^+ \delta_{n0} \tag{20b}$$

$$f_3^{(n+1)}(0) = \tau_{33}^{(n+1)}(0) = -q_3^- \delta_{n0} \tag{21a}$$

$$(n \geq 0)$$

$$f_3^{(n+1)}(a) = \tau_{33}^{(n+1)}(a) = -q_3^+ \delta_{n0} \tag{21b}$$

$$g_4^{(n+1)}\left[{}^{(i)}a\right] = \varphi^{(n+1)}\left[{}^{(i)}a\right] = {}^{(i)}V\,\delta_{n0}$$

$$(i = 0, \ldots, r+1) \quad (n \geq 0) \tag{22}$$

Substitution of Eq. (16) into Eq. (6) leads to the following simple recurrence relations:

$$\partial_z \boldsymbol{g}^{(0)} = \boldsymbol{0} \tag{23a}$$

$$\partial_z \boldsymbol{f}^{(n)} = \boldsymbol{A}\boldsymbol{g}^{(n)} \qquad (n \geq 0) \tag{23b}$$

$$\partial_z \boldsymbol{g}^{(n+1)} = \boldsymbol{B}\boldsymbol{f}^{(n)} \qquad (n \geq 0) \tag{23c}$$

A solution can be obtained by successively integrating these differential equations with respect to z and using Eqs. (17–22), i.e.,

$$\boldsymbol{g}^{(0)} = \begin{bmatrix} 0 \\ 0 \\ U_3^{(0)} \\ 0 \end{bmatrix} \tag{24}$$

$$\boldsymbol{f}^{(n)} = \begin{bmatrix} U_1^{(n)} \\ U_2^{(n)} \\ -q_3^- \delta_{n1} \\ D_0^{(n)} \end{bmatrix} + \boldsymbol{Q}\boldsymbol{A}\boldsymbol{g}^{(n)} + \begin{bmatrix} 0 \\ 0 \\ 0 \\ \sum_{j=1}^{r} {}^{(j)}\Delta D_3^{(n)} H\left[z - {}^{(j)}a\right] \end{bmatrix}$$

$$(n \geq 0) \tag{25}$$

$$\boldsymbol{g}^{(n+1)} = \begin{bmatrix} q_1^- \delta_{n0} \\ q_2^- \delta_{n0} \\ U_3^{(n+1)} \\ {}^{(0)}V\,\delta_{n0} \end{bmatrix} + \boldsymbol{Q}\boldsymbol{B}\boldsymbol{f}^{(n)} \qquad (n \geq 0) \tag{26}$$

where we denote the basic unknowns, the components of expansions of three mechanical displacements and the electric displacement at the lower surface $z = 0$ of the plate, as

$$U_\omega^{(n)} \equiv u_\omega^{(n)}(x_\rho, 0), \quad U_3^{(n)} \equiv u_3^{(n)}(x_\rho, 0), \quad D_0^{(n)} \equiv D_3^{(n)}(x_\rho, 0^+) \tag{27}$$

and the electric displacement jump across the jth internal electrode as

$${}^{(j)}\Delta D_3^{(n)} \equiv D_3^{(n)}\left[x_\rho, {}^{(j)}a^+\right] - D_3^{(n)}\left[x_\rho, {}^{(j)}a^-\right] \qquad (j = 1, \ldots, r) \tag{28}$$

with $H[z - {}^{(j)}a]$ being the Heaviside step function and

$$Q(\ldots) \equiv \int_0^z (\ldots)\,\mathrm{d}z \tag{29}$$

Because of the presence of internal electrodes, the transverse electric displacement is not continuous across each of the internally electroded surfaces, and the continuity condition for the transverse electric displacement at $z = {}^{(i)}a$ must be modified. However, here we specify the electric potential $\varphi[{}^{(i)}a]$. We include the electric displacement jumps [Eq. (28)] in the expression (25) after the integration of Eq. (23b) with respect to z.

Most plate theories implicitly designate the midplane of a plate to be the reference plane, and hence the basic unknowns are those at the midplane. It is clear, however, that at least four components of the unknown functions $\boldsymbol{F}$ and $\boldsymbol{G}$ will be known a priori when we choose either of the bounding plate surfaces to be the reference plane. Accordingly, the problem will be reduced to determining the remaining components of the unknown functions. For the specific problem the basic unknowns are chosen as the mechanical and electrical displacements on the bottom-most surface of the plate, i.e., Eq. (27). These unknowns are determined such that conditions (13–15) for the tractions and the electric potential on the top-most surface $z = a$ and for the electric potential at the internal electrodes are satisfied.

Substituting the expression (26) for $\boldsymbol{g}^{(n)}$ into Eq. (25) and simplifying the result, we obtain

$$\boldsymbol{f}^{(n)} = \boldsymbol{X}^{(n)} + \boldsymbol{H}^{(n)} + \begin{bmatrix} 0 \\ 0 \\ 0 \\ \sum_{j=1}^{r} {}^{(j)}\Delta D_3^{(n)} H\left[z - {}^{(j)}a\right] \end{bmatrix} \tag{30}$$

where

$$\boldsymbol{X}^{(n)} = \begin{bmatrix} U_1^{(n)} - z\partial_1 U_3^{(n)} \\ U_2^{(n)} - z\partial_2 U_3^{(n)} \\ 0 \\ D_0^{(n)} \end{bmatrix} \tag{31a}$$

$$\boldsymbol{H}^{(n)} = \delta_{n1}\left\{ \boldsymbol{Q}\boldsymbol{A}\begin{bmatrix} q_1^- \\ q_2^- \\ 0 \\ {}^{(0)}V \end{bmatrix} - \begin{bmatrix} 0 \\ 0 \\ q_3^- \\ 0 \end{bmatrix} \right\} + \boldsymbol{Q}\boldsymbol{A}\boldsymbol{Q}\boldsymbol{B}\boldsymbol{f}^{(n-1)} \tag{31b}$$

With expressions (30) and (31b), we obtain the following recurrence relation for the auxiliary function $\boldsymbol{H}^{(n)}$:

$$\boldsymbol{H}^{(n+1)} = \delta_{n0}\left\{ \boldsymbol{Q}\boldsymbol{A}\begin{bmatrix} q_1^- \\ q_2^- \\ 0 \\ {}^{(0)}V \end{bmatrix} - \begin{bmatrix} 0 \\ 0 \\ q_3^- \\ 0 \end{bmatrix} \right\}$$

$$+ \boldsymbol{Q}\boldsymbol{A}\boldsymbol{Q}\boldsymbol{B}\left\{ \boldsymbol{X}^{(n)} + \boldsymbol{H}^{(n)} + \begin{bmatrix} 0 \\ 0 \\ 0 \\ \sum_{j=1}^{r} {}^{(j)}\Delta D_3^{(n)} H\left[z - {}^{(j)}a\right] \end{bmatrix} \right\} \tag{32}$$

with the leading term $\boldsymbol{H}^{(0)} = \boldsymbol{0}$. Note that $\boldsymbol{H}^{(n)}$ contributes to the higher-order effective load terms in our asymptotic equations to be given later.

With the notation

$${}^{(i)}Q(\ldots) \equiv \int_0^{{}^{(i)}a} (\ldots)\,\mathrm{d}z \qquad (i = 1, \ldots, r+1) \tag{33}$$

and in particular

$$\bar{Q}(\ldots) \equiv \int_0^a (\ldots)\,\mathrm{d}z \qquad \text{or} \qquad \bar{Q} \equiv {}^{(r+1)}Q \tag{34}$$

and using Eq. (26), conditions (22) for the electric potentials specified on the internal electrodes and the upper surface of the plate can be written as

$${}^{(i)}Q\,B_{4L}\,f_L^{(n)} = \left[{}^{(i)}V - {}^{(0)}V\right]\delta_{n0} \qquad (i = 1, \ldots, r+1) \tag{35}$$

where an uppercase subscript L takes values from 1 to 4 and the usual summation convention applies to L. Furthermore, by using Eq. (30) and the relation

$$Q(\ldots)H[z-{}^{(j)}a]=H[z-{}^{(j)}a][Q-{}^{(j)}Q](\ldots) \qquad [{}^{(j)}a\geq 0] \tag{36}$$

Eq. (35) for $i=2,\ldots,r+1$ may be written in an alternative form as

$${}^{(i+1)}QB_{4L}[X_L^{(n)}+H_L^{(n)}]+\sum_{j=1}^{i}C_{ij}\,{}^{(j)}\Delta D_3^{(n)}=[{}^{(i+1)}V-{}^{(0)}V]\delta_{n0} \qquad (i=1,\ldots,r) \tag{37}$$

where C_{ij} is a lower-triangular matrix defined by

$$C_{ij}=\begin{cases}[{}^{(i+1)}Q-{}^{(j)}Q]B_{44} & (i\geq j)\\ 0 & (i<j)\end{cases} \tag{38}$$

Note that $B_{44}=N^{22}$ is only related to the material moduli depending on x_3, and thus (C_{ij}) is a constant matrix. Equation (37) may be viewed as a set of r linear algebraic equations for the electric displacement jumps ${}^{(j)}\Delta D_3^{(n)}$, which, using the property that the inverse of a lower-triangular matrix is also a lower-triangular matrix, give the expression

$${}^{(j)}\Delta D_3^{(n)}=\sum_{k=1}^{j}C_{jk}^{-1}\{[{}^{(k+1)}V-{}^{(0)}V]\delta_{n0}-{}^{(k+1)}QB_{4L}[X_L^{(n)}+H_L^{(n)}]\} \qquad (j=1,\ldots,r) \tag{39}$$

The upper surface traction conditions (20b) and (21b) may be alternatively expressed through Eqs. (25) and (26) as

$$\bar{Q}B_{\alpha L}f_L^{(n)}=(q_\alpha^+-q_\alpha^-)\delta_{n0} \tag{40}$$

$$\bar{Q}A_{3L}g_L^{(n+1)}=-(q_3^+-q_3^-)\delta_{n0} \tag{41}$$

Further using Eqs. (26) and (40) and noting $A_{3\alpha}=-\partial_\alpha$ and $A_{33}=A_{34}=0$, Eq. (41) can be written as

$$\bar{Q}zB_{\alpha L}\partial_\alpha f_L^{(n)}=[-(q_3^+-q_3^-)+a\partial_\alpha q_\alpha^+]\delta_{n0} \tag{42}$$

By using Eq. (36) and the expression obtained by substituting Eq. (39) into Eq. (30), we can write Eqs. (40), (42), and (35) for $i=1$ in the form of the matrix equation

$$\tilde{\boldsymbol{R}}\tilde{\boldsymbol{X}}^{(n)}[\equiv \boldsymbol{R}\boldsymbol{X}^{(n)}]=\delta_{n0}\boldsymbol{Y}-\boldsymbol{R}\boldsymbol{H}^{(n)} \tag{43}$$

where

$$\tilde{\boldsymbol{X}}^{(n)}=[U_1^{(n)}\quad U_2^{(n)}\quad U_3^{(n)}\quad D_0^{(n)}]^T \tag{44}$$

$$\tilde{R}_{\alpha\omega}=R_{\alpha\omega}=-\left\{\bar{Q}L_{\beta\rho}^{\alpha\omega}+\sum_{j=1}^{r}\sum_{k=1}^{j}C_{jk}^{-1}[\bar{Q}-{}^{(j)}Q]M_\beta^{\alpha 2\,(k+1)}QM_\rho^{\omega 2}\right\}\partial_\beta\partial_\rho$$

$$\tilde{R}_{\alpha 3}=\left\{\bar{Q}zL_{\beta\rho}^{\alpha\omega}+\sum_{j=1}^{r}\sum_{k=1}^{j}C_{jk}^{-1}[\bar{Q}-{}^{(j)}Q]M_\beta^{\alpha 2\,(k+1)}QzM_\rho^{\omega 2}\right\}\partial_\beta\partial_\omega\partial_\rho$$

$$R_{\alpha 3}=-\left\{\bar{Q}M_\beta^{\alpha 1}-\sum_{j=1}^{r}\sum_{k=1}^{j}C_{jk}^{-1}[\bar{Q}-{}^{(j)}Q]M_\beta^{\alpha 2\,(k+1)}QN^{21}\right\}\partial_\beta$$

$$\tilde{R}_{\alpha 4}=R_{\alpha 4}=-\left\{\bar{Q}M_\beta^{\alpha 2}-\sum_{j=1}^{r}\sum_{k=1}^{j}C_{jk}^{-1}[\bar{Q}-{}^{(j)}Q]M_\beta^{\alpha 2\,(k+1)}QN^{22}\right\}\partial_\beta$$

$$\tilde{R}_{3\omega}=R_{3\omega}=-\left\{\bar{Q}zL_{\beta\rho}^{\alpha\omega}+\sum_{j=1}^{r}\sum_{k=1}^{j}C_{jk}^{-1}[\bar{Q}-{}^{(j)}Q]zM_\beta^{\alpha 2\,(k+1)}QM_\rho^{\omega 2}\right\}\partial_\alpha\partial_\beta\partial_\rho$$

$$\tilde{R}_{33}=\left\{\bar{Q}z^2L_{\beta\rho}^{\alpha\omega}+\sum_{j=1}^{r}\sum_{k=1}^{j}C_{jk}^{-1}[\bar{Q}-{}^{(j)}Q]zM_\beta^{\alpha 2\,(k+1)}QzM_\rho^{\omega 2}\right\}\partial_\alpha\partial_\beta\partial_\omega\partial_\rho$$

$$R_{33}=-\left\{\bar{Q}zM_\beta^{\alpha 1}-\sum_{j=1}^{r}\sum_{k=1}^{j}C_{jk}^{-1}[\bar{Q}-{}^{(j)}Q]zM_\beta^{\alpha 2\,(k+1)}QN^{21}\right\}\partial_\alpha\partial_\beta$$

$$\tilde{R}_{34}=R_{34}=-\left\{\bar{Q}zM_\beta^{\alpha 2}-\sum_{j=1}^{r}\sum_{k=1}^{j}C_{jk}^{-1}[\bar{Q}-{}^{(j)}Q]zM_\beta^{\alpha 2\,(k+1)}QN^{22}\right\}\partial_\alpha\partial_\beta$$

$$\tilde{R}_{4\omega}=R_{4\omega}=-{}^{(1)}QM_\beta^{\omega 2}\partial_\beta, \qquad \tilde{R}_{43}={}^{(1)}QzM_\beta^{\omega 2}\partial_\beta\partial_\omega$$

$$R_{43}={}^{(1)}QN^{21}, \qquad \tilde{R}_{44}=R_{44}={}^{(1)}QN^{22} \tag{45}$$

$$Y_\alpha=q_\alpha^+-q_\alpha^-+\sum_{j=1}^{r}\sum_{k=1}^{j}C_{jk}^{-1}[\bar{Q}-{}^{(j)}Q]M_\beta^{\alpha 2}\partial_\beta[{}^{(k+1)}V-{}^{(0)}V]$$

$$Y_3=-(q_3^+-q_3^-)+a\partial_\alpha q_\alpha^+ +\sum_{j=1}^{r}\sum_{k=1}^{j}C_{jk}^{-1}[\bar{Q}-{}^{(j)}Q]zM_\beta^{\alpha 2}\partial_\alpha\partial_\beta[{}^{(k+1)}V-{}^{(0)}V]$$

$$Y_4={}^{(1)}V-{}^{(0)}V \tag{46}$$

Equation (43) is the key field equation obtained through our field asymptotic approach, from which the unknowns (44) of each order can be solved with specified edge conditions, material parameters, and loads. Equation (43) shows that $\boldsymbol{Y}$ is only related to the field equation at the leading-order ($n=0$), whereas $\boldsymbol{H}^{(n)}$ only contributes to the higher-order field equations because $\boldsymbol{H}^{(0)}=\boldsymbol{0}$, as mentioned earlier. However, $\boldsymbol{Y}$ is known a priori from Eq. (46); therefore, the leading-order unknowns can be determined from the leading-order field equation, i.e., from the so-called classical equation generalized to piezoelectric plates under prescribed surface and internal electric potentials as well as mechanical loads. Then $\boldsymbol{H}^{(1)}$ can be obtained from Eq. (32) by use of Eqs. (31a) and (39), and hence the unknowns for $n=1$ can be solved from the associated field equation of the corresponding order. Such a procedure may be continued to compute higher-order solutions, which may be considered as corrections to the so-called classical solution.

The differential operator $\tilde{\boldsymbol{R}}$ given by Eq. (45) for the field equations (43) of all orders may be recognized, when degenerated from piezoelectricity to pure elasticity, as being identical with that of the classical plate theory[41] for the bending of a thin monoclinic plate or laminate. Moreover, the matrix operators $\tilde{\boldsymbol{R}}$ and $\boldsymbol{R}$ in Eq. (43) have the same form for the field equations of all orders. Apart from $\boldsymbol{Y}$, which is nontrivial only for the leading order, the effective loads on the right-hand sides of Eq. (43) only involve derivatives of the auxiliary function $\boldsymbol{H}^{(n)}$ with respect to x_α and its integration with respect to z. The auxiliary function of higher order may be obtained from its preceding-order solution from Eqs. (32) and (39).

Note that expressions (39) give jumps in the electric displacement terms of other relevant physical quantities of the same order. Thus the order of field equations and the number of unknowns are not increased. When no internal electrodes are present, Eq. (39) and all terms involving summations in Eqs. (45) and (46) are discarded. It is possible to apply this technique to problems of composite laminates with weakened interfaces and delamination.

IV. Numerical Results and Discussion

To illustrate the aforestated asymptotic method, we consider a rectangular piezoelectric plate with its edges simply supported and grounded at $x_1=0, a$ and $x_2=0, b$, i.e.,

$$u_2=u_3=\tau_{11}=\varphi=0 \quad \text{at} \quad x_1=0,a$$
$$u_1=u_3=\tau_{22}=\varphi=0 \quad \text{at} \quad x_2=0,b \tag{47}$$

The mechanical and electric loadings are specified as

$$q_1^{\pm} = \hat{q}_1^{\pm} \cos l_1 x_1 \sin l_2 x_2$$

$$q_2^{\pm} = \hat{q}_2^{\pm} \sin l_1 x_1 \cos l_2 x_2$$

$$q_3^{\pm} = \hat{q}_3^{\pm} \sin l_1 x_1 \sin l_2 x_2$$

$$^{(i)}V = {}^{(i)}\hat{V} \sin l_1 x_1 \sin l_2 x_2 \qquad (i = 0, \ldots, r+1) \tag{48}$$

$$l_1 = m_1 \pi / a, \qquad l_2 = m_2 \pi / b \tag{49}$$

where a quantity with a superimposed hat denotes the amplitude of the corresponding physical quantity. Various quantities may not assume their maximum values at the same location.

The pointwise edge conditions (47) can be satisfied by assuming

$$\bar{\boldsymbol{X}}^{(n)} = \begin{bmatrix} U_1^{(n)} \\ U_2^{(n)} \\ U_3^{(n)} \\ D_0^{(n)} \end{bmatrix} = \begin{bmatrix} \hat{U}_1^{(n)} \cos l_1 x_1 \sin l_2 x_2 \\ \hat{U}_2^{(n)} \sin l_1 x_1 \cos l_2 x_2 \\ \hat{U}_3^{(n)} \sin l_1 x_1 \sin l_2 x_2 \\ \hat{D}_0^{(n)} \sin l_1 x_1 \sin l_2 x_2 \end{bmatrix} \tag{50}$$

A solution of each order may be obtained in the way described earlier and numerical results computed to any desired degree of accuracy for the specific problem.

The materials used in the paper are fiber-reinforced composite[30] (FRC), lead zirconate titanate[42] (PZT-4), and polyvinylidene fluoride[43] (PVDF). The material moduli of FRC, PZT-4, and PVDF are shown in Table 1, where ε_0 is the permittivity of vacuum. Because a linear theory is used, results for complex loadings can be obtained by a superposition of respective results in relation to simple loadings. Two loading conditions are examined in the following three numerical examples. One corresponds to applied normal tractions with vanishing electric potentials and another to applied electric potentials with vanishing normal tractions. For both cases $m_1 = m_2 = 1$ is used, and shear tractions on the top-most and bottom-most surfaces are set equal to zero, i.e., $q_\alpha^{\pm} = 0$. The mechanical and electric quantities are nondimensionalized by

$$\bar{u}_i = u_i / Pa, \qquad \bar{\tau}_{ij} = \tau_{ij} / Pc^*$$

$$\bar{\varphi} = e^* \varphi / Pac^*, \qquad \bar{D}_i = D_i / Pe^* \tag{51}$$

with $c^* = 1\ \mathrm{N/m^2}$, $e^* = 1\ \mathrm{C/m^2}$, and either $P = \hat{q}_3 / c^*$ for applied mechanical load $-q_3$ or $P = \hat{V}(e^*/ac^*)$ for applied electric potential V.

Table 1 Material moduli

Moduli	FRC	PZT-4	PVDF
c_{1111}, GPa	134.86	139	238.24
c_{2222}, GPa	14.352	139	23.6
c_{3333}, GPa	14.352	115	10.64
c_{1122}, GPa	5.1563	77.8	3.98
c_{1133}, GPa	5.1563	74.3	2.19
c_{2233}, GPa	7.1329	74.3	1.92
c_{2323}, GPa	3.606	25.6	2.15
c_{3131}, GPa	5.654	25.6	4.4
c_{1212}, GPa	5.654	30.6	6.43
e_{311}, C/m^2	0	−5.2	−0.13
e_{322}, C/m^2	0	−5.2	−0.145
e_{333}, C/m^2	0	15.1	−0.276
e_{223}, C/m^2	0	12.7	−0.009
e_{113}, C/m^2	0	12.7	−0.135
$\varepsilon_{11}/\varepsilon_0$[a]	3.5	1475	12.5
$\varepsilon_{22}/\varepsilon_0$[a]	3.0	1475	11.98
$\varepsilon_{33}/\varepsilon_0$[a]	3.0	1300	11.98

[a] $\varepsilon_0 = 8.854185$ pF/m.

A. Hybrid Laminate

In the first example results obtained from the aforestated asymptotic approach are compared with those obtained from the exact solution.[30] A two-ply (0 deg/90 deg) piecewise homogeneous FRC laminate with the 0-deg lamina on the top is perfectly bonded between two homogeneous PZT-4 piezoelectric layers. Thicknesses of the PZT-4 lamina and the FRC lamina equal $0.1h$ and $0.4h$, respectively. The hybrid laminate ($a/b = 1$, $a/h = 4$) without internal electrodes is subjected to normal traction q_3^+ and electric potential $^{(1)}V$ on the upper surface. Some selected results are given in Table 2, together with the exact values.[30] The order of the present solution is increased from 0 to 40. In addition, the repeated averaging technique for n partial sums (denoted as n term RA in Table 2) is used to accelerate the convergence of the asymptotic results. The technique can be shown to be a special case of Euler's transformation; more details may be found, for example, in the book.[44]

The present asymptotic solution for the applied mechanical loading converges more rapidly than that for the applied electric loading. The second-order approximation for the applied mechanical loading is quite good with an error of less than 2%. However, this is not the case for the applied electric loading. The error in the 10th-order aproximation for the applied potential is more than 10% when these results are compared with 10th-order results obtained by using five-term repeated averaging. Furthermore, even for the 40th-order solution, the value of $\bar{\tau}_{13}$ changes in the third significant digit. However, the 6th-order solution obtained by using three-term repeated averaging is better than 10th- and 30th-order approximation for applied mechanical and electric loadings, respectively. Numerical convergence is reached at least to four significant digits for the 10th-order results with five-term repeated averaging, which are in excellent agreement with the exact solution.[30] In principle, results can be computed to any desired degree of accuracy for a specific problem by the present method; thus, the technique gives a pseudoexact solution in this sense. The slight difference between our and Heyliger's[30] results is possibly caused by different truncation errors in the two studies. In the results given in Figs. 1–6 and Table 3, the repeated averaging technique is used to achieve the desired accuracy.

B. Two-Layer Laminate of Dissimilar Piezoelectric Materials

A two-layer laminate of dissimilar piezoelectric materials PZT-4/PVDF with PZT-4 on the top is considered in this example to show

Table 2 Comparison of the present solutions of different orders with exact results for a hybrid laminate ($a/b = 1$, $a/h = 4$)

	Applied mechanical load		Applied electric potential	
Order	$\bar{\tau}_{33}(x_3 = h/2)$	$\bar{D}_3(x_3 = 0)$	$\bar{u}_1(x_3 = 0)$	$\bar{\tau}_{13}(x_3 = h/2)$
0	0	−4.7548e−20	−8.3668e−14	0
1	0.50000	−1.3428e−11	−4.7860e−12	0.005044
2	0.50542	−1.4512e−11	−1.2417e−12	−0.167291
10	0.49812	−1.4231e−11	−2.5393e−12	−0.108143
20	0.49827	−1.4242e−11	−2.8202e−12	−0.097068
30	0.49829	−1.4243e−11	−2.8565e−12	−0.095635
39	0.49829	−1.4244e−11	−2.8628e−12	−0.095388
40	0.49829	−1.4244e−11	−2.8612e−12	−0.095449
6 (3 term-RA)	0.49819	−1.4242e−11	−2.8623e−12	−0.095299
10 (5 term-RA)	0.49830	−1.4246e−11	−2.8617e−12	−0.095419
Exact[30]	0.49831	−1.4246e−11	−2.8625e−12	−0.095464

Table 3 Dimensionless midplane central deflection and central electric displacement jumps across internal electrodes for an actuated laminate ($a/b = 1$)

a/h	$10^8 \times \bar{u}_3(0.5h)$	$10^6 \times \Delta\bar{D}_3(0.5h \pm 0.4h)$
4	0.2349	−0.6128
10	1.4166	−1.5338
20	5.6341	−3.0682
50	35.1561	−7.6709

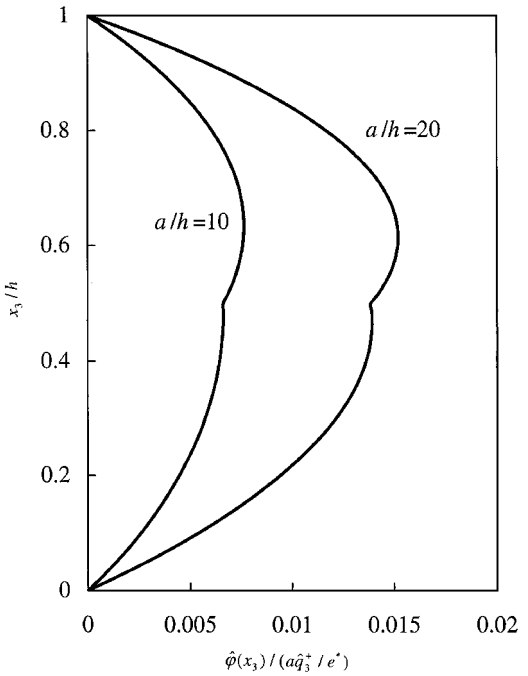

Fig. 1 Through-the-thickness distribution of the amplitude of the dimensionless electric potential for a PZT-4/PVDF laminate under mechanical load q_3^+ ($a/b = 1$).

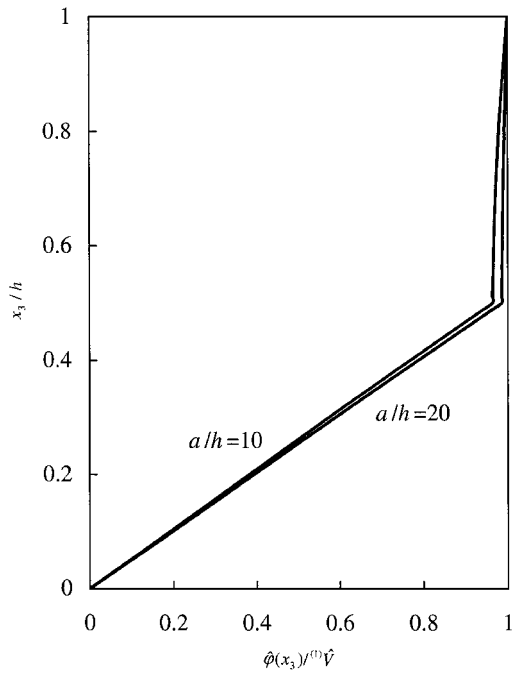

Fig. 2 Through-the-thickness distribution of the amplitude of the dimensionless electric potential for a PZT-4/PVDF laminate under electric load $^{(1)}V$ ($a/b = 1$).

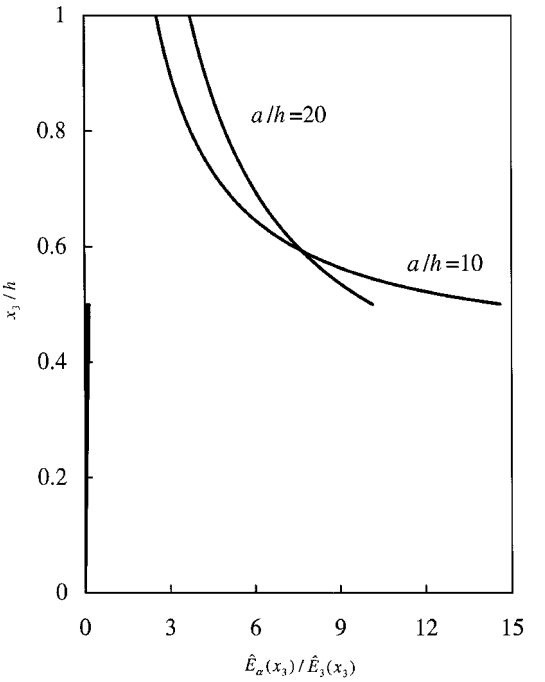

Fig. 3 Through-the-thickness distribution of the amplitude ratio of the in-plane to out-of-plane electric field components for a PZT-4/PVDF laminate under electric load $^{(1)}V$ ($a/b = 1$).

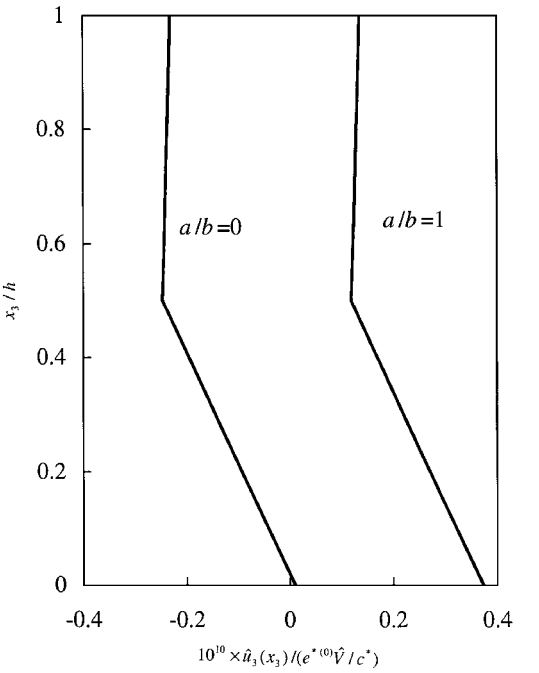

Fig. 4 Through-the-thickness distribution of the amplitude of the dimensionless out-of-plane mechanical displacement for a PZT-4/PVDF laminate under electric load $^{(0)}V$ ($a/h = 10$).

possible deficiencies in the existing two-dimensional piezoelectric plate models. Each lamina is homogeneous and of equal thickness. The aspect ratio is taken as $a/b = 1$ in Figs. 1–3 and $a/b = 0$, 1 in Fig. 4. The span-to-thickness ratio is taken as $a/h = 10$, 20 in Figs. 1–3, and $a/h = 10$ in Fig. 4. The only nonzero surface loading is q_3^+ applied on the upper surface for results presented in Fig. 1, $^{(1)}V$ applied on the upper surface for results given in Figs. 2 and 3, and $^{(0)}V$ applied on the lower surface for results exhibited in Fig. 4. No internal electrodes are present.

The dimensionless amplitude of the through-thickness electric potential for the two-layer PZT-4/PVDF laminate is presented in Fig. 1 for the applied mechanical load and in Fig. 2 for the applied

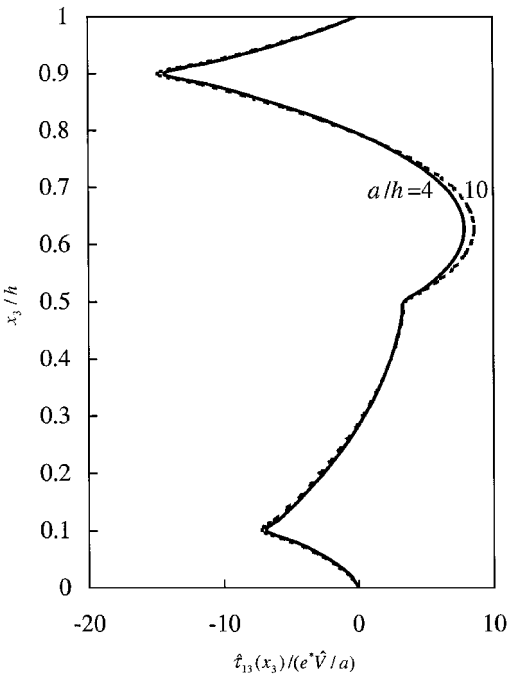

Fig. 5 Through-the-thickness distribution of the amplitude of the dimensionless transverse shear stress for a smart plate element ($a/b = 1$).

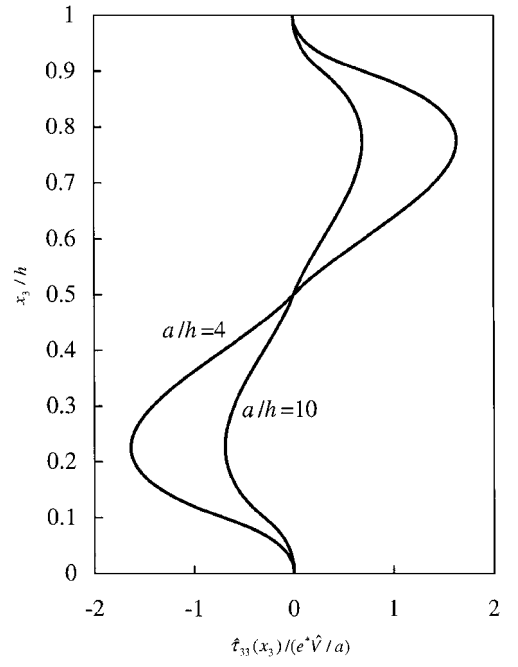

Fig. 6 Through-the-thickness distribution of the amplitude of the dimensionless transverse normal stress for a smart plate element ($a/b = 1$).

electric potential. As expected, the electric potential distributions in Figs. 1 and 2 are nonlinear through the thickness for both moderately thick ($a/h = 10$) and thin ($a/h = 20$) laminates. Therefore, the usual assumption, made in existing piezoelectric laminate theories, that the electric potential is represented by a continuously differentiable function through-the-plate thickness is not appropriate. However, it is more reasonable to model the electric potential by assuming a piecewise quadratic distribution for the applied mechanical load case (see Fig. 1) and a piecewise linear distribution for the applied potential case (see Fig. 2). In the three-layer cross-ply simply supported square plate with the stacking sequence [0/90/0] made of PVDF, Heyliger[31] found that the through-thickness distribution of the electric potential is nearly parabolic when normal tractions are applied on the top and/or bottom surfaces of the plate. However, it is almost linear when an electric potential is applied across these surfaces. In each case the curve can be represented by a continuously differentiable function. Thus the through-thickness variation of the electric potential in a laminated piezoelectric plate depends upon the loads on its top and bottom surfaces, the stacking sequence, and the relative anisotropy of the adjoining laminae.

An exact analytical solution for a single-layer thin plate[45] has revealed that it is reasonable to neglect in-plane components of the electric field in some of two-dimensional thin piezoelectric plate theories if the transverse electric displacements on the upper and lower surfaces of a plate are equal. This is justified because the ratio of the in-plane to out-of-plane components of the electric field is of the order of the plate thickness parameter, which is a small quantity. However, for plates where the transverse electric displacements on the top and bottom surfaces are unequal, the thin piezoelectric plate models are not appropriate as they have neglected the in-plane electric field components, which, compared with the transverse electric field, are of the order of the reciprocal of the plate thickness parameter. This becomes clear from the numerical results given in Fig. 3, where the through-thickness distribution of the amplitude ratio of in-plane to out-of-plane electric field components $\hat{E}_\alpha/\hat{E}_3$, which is discontinous at the PZT-4/PVDF interface, is shown. We notice that although the in-plane electric field components are negligibly small in the PVDF layer they are more significant than the transverse electric field component in the PZT-4 layer. Consequently, the assumption of negligible in-plane electric field components is not valid.

Figure 4 shows the through-thickness distribution of the amplitude of the out-of-plane mechanical displacement. The distribution is approximately piecewise linear through the plate thickness. Thus the approximation of constant through-the-thickness distribution of the out-of-plane displacement made in existing two-dimensional piezoelectric plate theories is not satisfactory at least for a two-layer laminate of dissimilar piezoelectric materials.

C. Laminate with Affixed Actuators

The last example considers an elastic laminate with actuators bonded symmetrically to its top and bottom surfaces. This smart structural element is chosen to have the same configuration as the four-ply (PZT-4/0-deg FRC/90-deg FRC/PZT-4) hybrid laminate studied in the first example, and the distributions of the transverse shear stress and the normal stress through-the-plate thickness are examined for $a/h = 4$ and 10. Because the electric voltage is applied to the surfaces of an actuator, two internal conducting electrodes on the inner surfaces of the PZT-4 actuators are incorporated. Accordingly, four electrodes of vanishing thicknesses are present. The amplitudes of the electric potential on these electrodes are specified as $\hat{V}$, 0, 0, and $\hat{V}$ at $x_3 = 0$, $h/10$, $9h/10$, and h, respectively.

The dimensionless midplane central deflection and the jump in the central electric displacement across the internal electrodes for $a/h = 4$, 10, 20, and 50 are listed in Table 3. The midplane central deflection increases very rapidly as the thickness of the plate is decreased. The magnitude of the jump in the central electric displacement is essentially proportional to a/h for the four cases studied. The through-thickness distribution of the nondimensional transverse shear stress, depicted in Fig. 5, is virtually the same for $a/h = 4$ and 10, is continuous across the interfaces, and its maximum value occurs at the interface between the substrate and the top actuator. For the problem studied herein delamination will first occur at this interface. For two plates of equal thickness, the dimensional transverse shear stress will be inversely proportional to an in-plane dimension. However, the through-thickness distribution of the normal stress, exhibited in Fig. 6, is strongly influenced by the aspect ratio a/h of the plate. The boundary conditions at the top and bottom surfaces required that $\hat{\tau}_{33}$ vanish there, and the continuity of $\hat{\tau}_{33}$ across the interfaces is well satisfied. For a thick plate with $a/h = 4$, the magnitude of the normal stress is maximum at $x_3/h \simeq 0.225$ and 0.775.

V. Conclusions

We have presented an efficient and reliable asymptotic scheme that reduces a three-dimensional coupled electromechanical problem of a laminated piezoelectric plate to a hierarchy of two-dimensional plate equations that can be solved systematically without progressively increasing difficulty. The incorporation of internal electrodes into the analysis is one of the novel aspects and

enlarges the applicability of the present formulation to a wide range of practical problems. Numerical results show excellent agreement with available exact solutions and bring out some of the deficiencies in existing two-dimensional piezoelectric plate models. The method satisfied the continuity of surface tractions at the interfaces and can account for the jump in the normal electric displacement across the internal electrodes.

The computation of higher-order terms in the expansion requires the knowledge of the relevant boundary conditions,[26] which could be obtained by studying the boundary-layer effects along the contour of the plate. Admittedly, this is a difficult problem. However, by specifying the boundary conditions of each order on the reference plane of a plate, the solution in the interior of the plate is expected to be sufficiently satisfactory for most engineering problems.

Acknowledgments

This work was partially supported by Army Research Office Grant DAAG55-98-1-0030 and National Science Foundation Grant CMS9713453 to Virginia Polytechnic Institute and State University.

References

[1]Crawley, E. F., "Intelligent Structures for Aerospace: A Technology Overview and Assessment," *AIAA Journal*, Vol. 32, No. 8, 1994, pp. 1689–1699.

[2]Crawley, E. F., and de Luis, J., "Use of Piezoelectric Actuators as Elements of Intelligent Structures," *AIAA Journal*, Vol. 25, No. 10, 1987, pp. 1373–1385.

[3]Koconis, D. B., Kollár, L. P., and Springer, G. S., "Shape Control of Composite Plates and Shells with Embedded Actuators. I. Voltages Specified," *Journal of Composite Materials*, Vol. 28, No. 5, 1994, pp. 415–458.

[4]Koconis, D. B., Kollár, L. P., and Springer, G. S., "Shape Control of Composite Plates and Shells with Embedded Actuators. II. Desired Shape Specified," *Journal of Composite Materials*, Vol. 28, No. 5, 1994, pp. 459–482.

[5]Zhou, Y. S., and Tiersten, H. F., "Elastic Analysis of Laminated Composite Plates in Cylindrical Bending due to Piezoelectric Actuators," *Smart Materials and Structures*, Vol. 3, No. 3, 1994, pp. 255–265.

[6]Batra, R. C., Liang, X. Q., and Yang, J. S., "Shape Control of Vibrating Simply Supported Rectangular Plates," *AIAA Journal*, Vol. 34, No. 1, 1996, pp. 116–122.

[7]Batra, R. C., Liang, X. Q., and Yang, J. S., "The Vibration of a Simply Supported Rectangular Elastic Plate due to Piezoelectric Actuators," *International Journal of Solids and Structures*, Vol. 33, No. 11, 1996, pp. 1597–1618.

[8]Batra, R. C., and Liang, X. Q., "The Vibration of a Rectangular Laminated Elastic Plate with Embedded Piezoelectric Sensors and Actuators," *Computers and Structures*, Vol. 63, No. 2, 1997, pp. 203–216.

[9]Lee, C. K., "Theory of Laminated Piezoelectric Plates for the Design of Distributed Sensors/Acuators. Part I: Governing Equations and Reciprocal Relationships," *Journal of the Acoustical Society of America*, Vol. 87, No. 3, 1990, pp. 1144–1158.

[10]Wang, B. T., and Rogers, C. A., "Laminated Theory for Spatially Distributed Induced Strain Actuators," *Journal of Composite Materials*, Vol. 25, No. 4, 1991, pp. 433–453.

[11]Tauchert, T. R., "Piezothermoelastic Behavior of a Laminated Plate," *Journal of Thermal Stresses*, Vol. 15, No. 1, 1992, pp. 25–37.

[12]Yong, Y. K., Stewart, J. T., and Ballato, A., "A Laminated Plate Theory for High Frequency, Piezoelectric Thin-Film Resonators," *Journal of Applied Physics*, Vol. 74, No. 5, 1993, pp. 3028–3046.

[13]Tzou, H. S., *Piezoelectric Shells: Distributed Sensing and Control of Continua*, Kluwer Academic, Norwell, MA, 1993.

[14]Mitchell, J. A., and Reddy, J. N., "A Refined Hybrid Plate Theory for Composite Laminates with Piezoelectric Laminae," *International Journal of Solids and Structures*, Vol. 32, No. 16, 1995, pp. 2345–2367.

[15]Huang, J. H., and Wu, T. L., "Analysis of Hybrid Multilayered Piezoelectric Plates," *International Journal of Engineering Science*, Vol. 34, No. 2, 1996, pp. 171–181.

[16]Noor, A. K., and Burton, W. S., "Assessment of Shear Deformation Theories for Multilayered Composite Plates," *Applied Mechanics Reviews*, Vol. 42, No. 1, 1989, pp. 1–13.

[17]Reddy, J. N., and Robbins, D. H., Jr., "Theories and Computational Models for Composite Laminates," *Applied Mechanics Reviews*, Vol. 47, No. 6, 1994, pp. 147–169.

[18]Wang, Y. M., and Tarn, J. Q., "A Three-Dimensional Analysis of Anisotropic Inhomogeneous and Laminated Plates," *International Journal of Solids and Structures*, Vol. 31, No. 4, 1994, pp. 497–515.

[19]Tarn, J. Q., "An Asymptotic Theory for Dynamic Response of Anisotropic Inhomogeneous and Laminated Cylindrical Shells," *Journal of the Mechanics and Physics of Solids*, Vol. 42, No. 10, 1994, pp. 1633–1650.

[20]Tarn, J. Q., "Elastic Buckling of Multilayered Anisotropic Plates," *Journal of the Mechanics and Physics of Solids*, Vol. 44, No. 3, 1996, pp. 389–411.

[21]Tarn, J. Q., "An Asymptotic Variational Formulation for Dynamic Analysis of Multilayered Anisotropic Plates," *Computer Methods in Applied Mechanics and Engineering*, Vol. 130, Nos. 3–4, 1996, pp. 337–353.

[22]Tarn, J. Q., "An Asymptotic Theory for Nonlinear Analysis of Multilayered Anisotropic Plates," *Journal of the Mechanics and Physics of Solids*, Vol. 45, No. 7, 1997, pp. 1105–1120.

[23]Tarn, J. Q., and Wang, Y. M., "An Asymptotic Theory for Dynamic Response of Anisotropic Inhomogeneous and Laminated Plates," *International Journal of Solids and Structures*, Vol. 31, No. 2, 1994, pp. 231–246.

[24]Tarn, J. Q., and Wang, Y. M., "Asymptotic Thermoelastic Analysis of Anisotropic Inhomogeneous and Laminated Plates," *Journal of Thermal Stresses*, Vol. 18, No. 1, 1995, pp. 35–58.

[25]Tarn, J. Q., and Wang, Y. B., "A Refined Asymptotic Theory and Computational Model for Multilayered Composite Plates," *Computer Methods in Applied Mechanics and Engineering* , Vol. 145, Nos. 1–2, 1997, pp. 167–184.

[26]Maugin, G. A., and Attou, D., "An Asymptotic Theory of Thin Piezoelectric Plates," *Quarterly Journal of Mechanics and Applied Mathematics*, Vol. 43, No. 3, 1990, pp. 347–362.

[27]Bisegna, P., and Maceri, F., "A Consistent Theory of Thin Piezoelectric Plates," *Journal of Intelligent Material Systems and Structures*, Vol. 7, No. 4, 1996, pp. 372–389.

[28]Pagano, N. J., "Exact Solutions for Composite Laminates in Cylindrical Bending," *Journal of Composite Materials*, Vol. 3, No. 3, 1969, pp. 398–411.

[29]Pagano, N. J., "Exact Solutions for Rectangular Bi-Directional Composites and Sandwich Plates," *Journal of Composite Materials*, Vol. 4, No. 1, 1970, pp. 20–34.

[30]Heyliger, P., "Static Behavior of Laminated Elastic/Piezoelectric Plates," *AIAA Journal*, Vol. 32, No. 12, 1994, pp. 2481–2484.

[31]Heyliger, P., "Exact Solutions for Simply Supported Laminated Piezoelectric Plates," *Journal of Applied Mechanics*, Vol. 64, No. 2, 1997, pp. 299–306.

[32]Heyliger, P., and Brooks, S., "Exact Solutions for Laminated Piezoelectric Plates in Cylindrical Bending," *Journal of Applied Mechanics*, Vol. 63, No. 4, 1996, pp. 903–910.

[33]Nowotny, H., Benes, E., and Schmid, M., "Layered Piezoelectric Resonators with an Arbitrary Number of Electrodes (General One-Dimensional Treatment)," *Journal of the Acoustical Society of America*, Vol. 90, No. 3, 1991, pp. 1238–1245.

[34]Sosa, H. A., "On the Modeling of Piezoelectric Laminated Structures," *Mechanics Research Communications*, Vol. 19, No. 6, 1992, pp. 541–546.

[35]Stewart, J. T., and Yong, Y. K., "Exact Analysis of the Propagation of Acoustic Waves in Multilayered Anisotropic Piezoelectric Plates," *IEEE Transactions on Ultrasonics, Ferroelectrics, and Frequency Control*, Vol. 41, No. 3, 1994, pp. 375–390.

[36]Xu, K. M., Noor, A. K., and Tang, Y. Y., "Three-Dimensional Solutions for Coupled Thermoelectroelastic Response of Multilayered Plates," *Computer Methods in Applied Mechanics and Engineering*, Vol. 126, Nos. 3–4, 1995, pp. 355–371.

[37]Xu, K. M., Noor, A. K., and Tang, Y. Y., "Three-Dimensional Solutions for Free Vibrations of Initially-Stressed Thermoelectroelastic Multilayered Plates," *Computer Methods in Applied Mechanics and Engineering*, Vol. 141, Nos. 1–2, 1997, pp. 125–139.

[38]Lee, J. S., and Jiang, L. Z., "Exact Electroelastic Analysis of Piezoelectric Laminae via State Space Approach," *International Journal of Solids and Structures*, Vol. 33, No. 7, 1996, pp. 977–990.

[39]Tiersten, H. F., *Linear Piezoelectric Plate Vibrations*, Plenum, New York, 1969.

[40]Maugin, G. A., *Continuum Mechanics of Electromagnetic Solids*, North-Holland, Amsterdam, 1988.

[41]Reddy, J. N., *Mechanics of Laminated Composite Plates: Theory and Analysis*, CRC Press, Boca Raton, FL, 1997.

[42]Berlincourt, D. A., Curran, D. R., and Jaffe, H., "Piezoelectric and Piezomagnetic Materials and Their Function in Transducers," *Physical Acoustics*, Vol. 1, edited by W. P. Mason, Academic, New York, 1964, pp. 169–270.

[43]Tashiro, K., Tadokoro, H., and Kobayashi, M., "Structure and Piezoelectricity of Poly (Vinylidene Fluoride)," *Ferroelectrics*, Vol. 32, Nos. 1–4, 1981, pp. 167–175.

[44]Dahlquist, G., and Björck, Å., *Numerical Methods*, Prentice–Hall, Upper Saddle River, NJ, 1974.

[45]Bisegna, P., and Maceri, F., "An Exact Three-Dimensional Solution for Simply Supported Rectangular Piezoelectric Plates," *Journal of Applied Mechanics*, Vol. 63, No. 3, 1996, pp. 628–638.

A. M. Waas
Associate Editor